Atmospheric Environment 62 (2012) 492–501

Contents lists available at SciVerse ScienceDirect

Atmospheric Environment

journal homepage: www.elsevier.com/locate/atmosenv

Aircraft measurements of SO_2 and aerosols over northeastern China: Vertical profiles and the influence of weather on air quality

Can Li [a], Jeffrey W. Stehr [a], Lackson T. Marufu [a], Zhanqing Li [a,b,*], Russell R. Dickerson [a]

[a] Earth System Science Interdisciplinary Center and Department of Atmospheric and Oceanic Science, University of Maryland, College Park, MD, USA
[b] State Key Laboratory of Earth Surface Processes and Resource Ecology, GCESS, Beijing Normal University, Beijing 100875, China

HIGHLIGHTS

- Dramatic change in air quality caused by shift in weather pattern.
- Significant difference in aerosol properties between N China and E U.S.
- Prevalent dust layers in the free troposphere over N China.

ARTICLE INFO

Article history:
Received 27 February 2012
Received in revised form
30 July 2012
Accepted 31 July 2012

Keywords:
Aircraft measurements
SO_2
Aerosols
Vertical profile
Weather and air quality

ABSTRACT

Aircraft measurements of SO_2 and aerosol scattering coefficients (b_{sp}) were made over Shenyang, an industrialized city in northeastern China in April 2005. Weather conditions were found to have strong impact on the area's air quality. Between two flights on April 10 and 11, the SO_2 loading increased by an order of magnitude within 24 h, from ~0.1 DU (Dobson Unit) to ~1 DU. Meteorological observations and back trajectory analyses suggest that anthropogenic pollutants emitted from the area accumulated under stagnant conditions induced by a mid-latitude cyclone approaching from the west. The observed rapid buildup demonstrates that strong local emissions can expose the populace to high pollutant levels under unfavorable weather conditions. Ångström exponents determined from the aircraft and ground-based sun photometers are significantly smaller over China than over the U.S., suggesting the prevalence of dust particles in northern China, particularly in spring. The coarse mode became more pronounced with altitude, indicating dust-dominant aerosol layers in the lower free troposphere, which should be accounted for in the satellite remote sensing of surface pollution over the region. Information on the vertical distribution of aerosols and precursor gases over China will also help better understand their transport as well as effects on weather and climate.

1. Introduction

Shenyang, the capital of Liaoning Province in northeastern China, is a heavily industrialized city located about 600 km northeast of Beijing. Consuming more than ten million tons of coal every year (Hao et al., 2006), this city of over seven million residents was once among the most polluted cities in the world (He et al., 2002). Hence, drastic environmental measures were implemented in recent years to reduce emissions from major industrial sources. Locally, SO_2 and particulate matter (PM) have adverse effects on human health, as suggested by the positive association between daily mortality and pollutant levels in Shenyang (Xu et al., 2000). Regionally, pollutants emitted from the area can travel long distances under certain weather conditions, influencing regions thousands of kilometers downwind (e.g., Bey et al., 2001). Aerosols over Shenyang absorb solar radiation (e.g., Xia et al., 2007), and may exert impacts on weather and regional climate.

The vertical distribution of atmospheric pollutants is a critical factor determining their long-range transport (e.g., Li et al., 2010a), and should be accounted for in remote sensing of air pollution from space (e.g., Krotkov et al., 2008). Several aircraft campaigns (e.g., Jacob et al., 2003; Huebert et al., 2003; Parrish et al., 2004) have been carried out over the Western Pacific to characterize outflow from East Asia. Airborne measurements over mainland China are

* Corresponding author. State Key Laboratory of Earth Surface Processes and Resource Ecology, GCESS, Beijing Normal University, Beijing 100875, China. Tel.: +1 301 405 6699.
E-mail address: zli@atmos.umd.edu (Z. Li).

1352-2310/$ – see front matter © 2012 Published by Elsevier Ltd.
http://dx.doi.org/10.1016/j.atmosenv.2012.07.076

relatively scarce and reports on them have only recently become available (e.g., Hatakeyama et al., 2005; Ma et al., 2010; Wang et al., 2006, 2007; Zhang et al., 2006). Despite their limited spatial and temporal coverage, these flights were able to provide insight into the meteorological mechanisms for long-range transport of Asian pollution and dust. For example, Ding et al. (2009) observed the long-range transport of pollutants within the warm conveyer belt associated with a mid-latitude wave cyclone over northern China. Chen et al. (2009) described the ventilation of pollutants from the Beijing area through the mountain chimney effect. Airborne observations over China have also proved useful for evaluating and improving satellite retrievals (He et al., 2012; Krotkov et al., 2008; Xue et al., 2010).

In April 2005, an air campaign was carried out around Shenyang, under the auspices of EAST-AIRE, East Asian Study of Tropospheric Aerosols: an International Regional Experiment (Li et al., 2007a). Eight research flights were made under various synoptic conditions. In our previous study (Dickerson et al., 2007), two flights (April 5 and 7, 2005) were analyzed to reveal the role of dry (non-precipitating) convection in lifting pollutants out of the boundary layer over China. In this paper, we focus on the remaining six flights to shed more light on the vertical distribution of pollutants under diverse weather conditions, as well as on aerosol properties and their dependence on altitude.

2. Methodology

A modified Chinese Y-12 twin engine turboprop aircraft was used in this experiment. The Y-12 has a cruise speed of ~200 km h^{-1} and a ceiling of ~7000 m. A forward-facing isokinetic inlet mounted

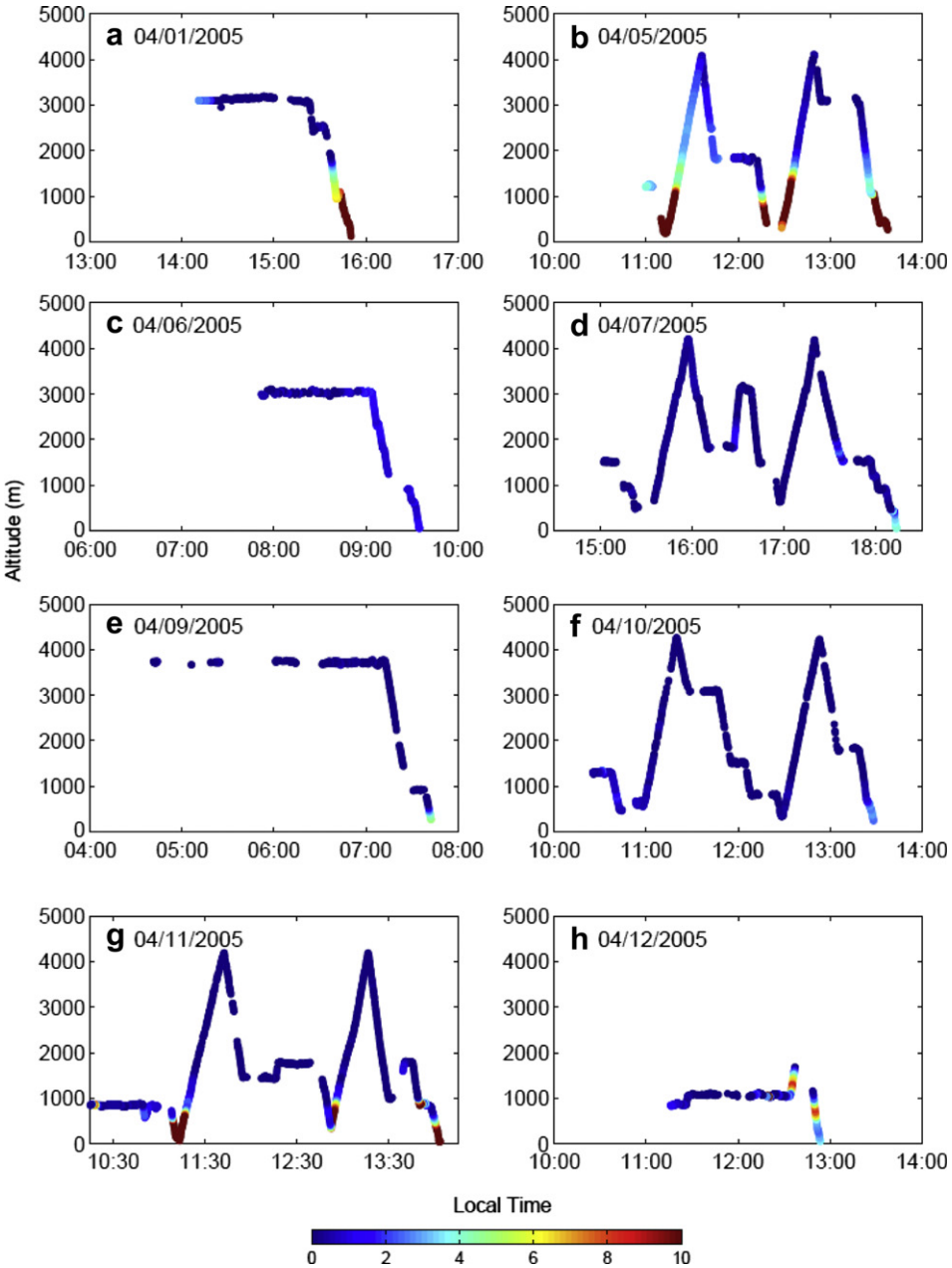

Fig. 1. SO_2 concentration (color, unit: ppbv) and flight altitude along the flight routes on April 1, 5, 6, 7, 9, 10, 11, and 12, 2005 over the Shenyang area. (For interpretation of the references to colour in this figure legend, the reader is referred to the web version of this article.)

on the top of the cockpit, ahead of the engines, collected samples for aerosol instruments. A backward-facing inlet installed at the same spot was used for trace gas instruments.

The University of Maryland (UMD) light aircraft instrument package mounted on the Y-12 has been previously described elsewhere (Taubman et al., 2004; Dickerson et al., 2007) and is only briefly introduced in this paper. Ozone was measured with a commercial UV absorption instrument (Thermo Environmental Instruments Model 49, Franklin, MA). For SO_2, we used a modified (Luke, 1997) commercial pulsed-fluorescence detector (Thermo Environmental Instruments Model 43C). Aerosol scattering coefficients at three wavelengths (450, 550, and 700 nm) were determined using an integrating nephelometer (TSI Model 3563, Shoreview, MN). The non-ideal forward-scattering truncation of the nephelometer was corrected for following the Anderson and Ogren (1998) method. A RH/T probe (EIL Instruments Inc. Rustrak RR2-252, Hunt Valley, MD) measured ambient temperature and relative humidity. A Rosemount Model 2008 pressure transducer provided information regarding ambient pressure. Flight positions were recorded with a Global Positioning System instrument (Garmin GPS-90).

During the experiment, the Y-12 aircraft was deployed at the Taoxian International Airport (41.640°N 123.488°E), ~20 km south-southeast of downtown Shenyang. Besides Shenyang, five other cities with population of 400,000 or more (Fushun, Benxi, Liaoyang, Tieling, and Anshan) lie within 80 km from the airport. The region is also heavily industrialized, with numerous factories of automotive, chemical, mechanic, power, and steel industries emitting substantial amounts of pollutants.

Ground-based AERONET (AErosol RObotic NETwork) observations of aerosols were made at a site ~70 km southwest of downtown Shenyang (Liaozhong: 41.512°N, 122.701°E), and ~20 km away from the south profiling locations during the campaign. The

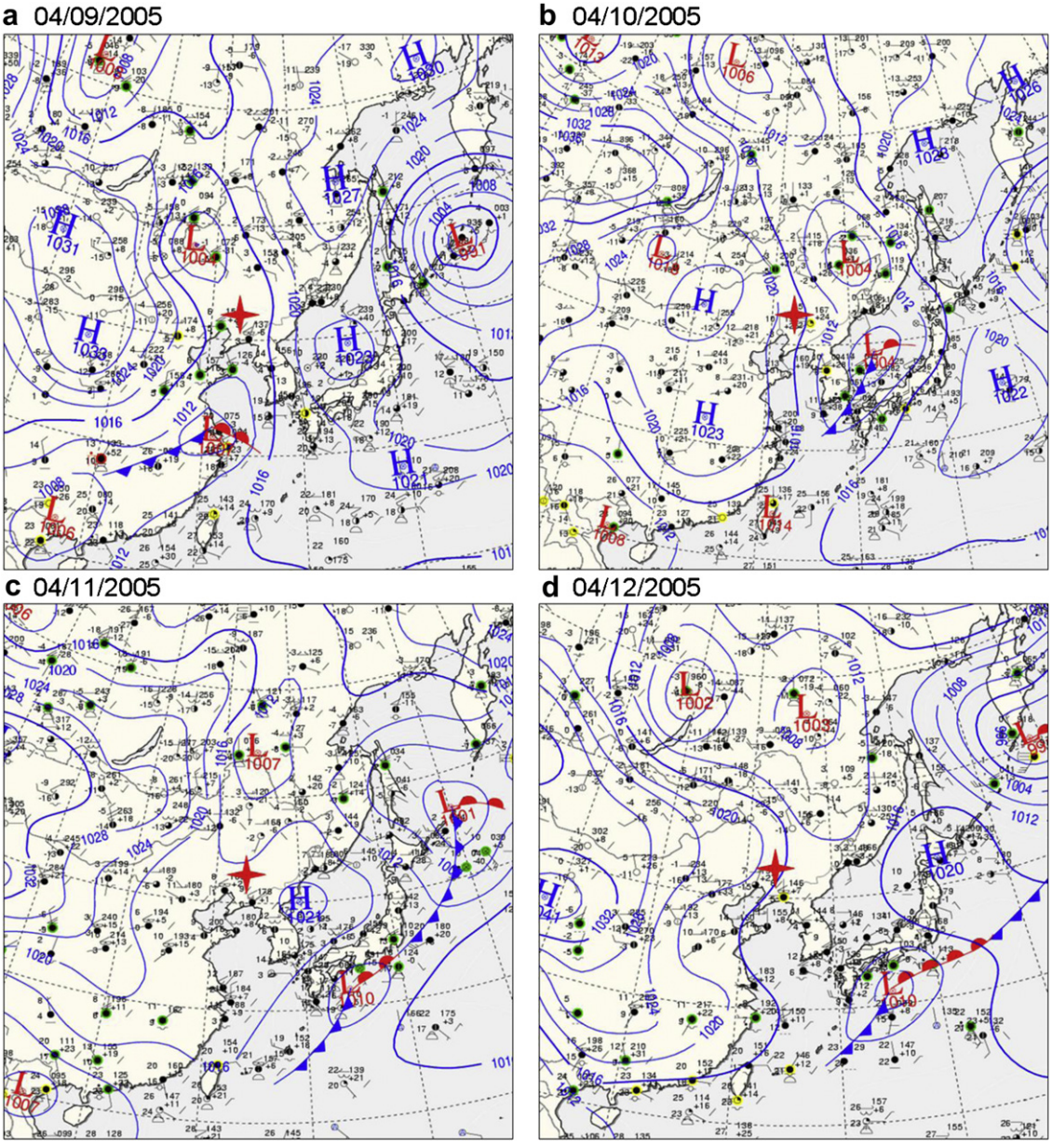

Fig. 2. Surface weather maps for East Asia from April 9 to 12, 2005 (source: Korean Meteorological Agency). The campaign area is approximately marked by red stars. (For interpretation of the references to colour in this figure legend, the reader is referred to the web version of this article.)

AERONET program (Holben et al., 1998) is a federation of ground-based remote sensing aerosol networks operating hundreds of sun photometers around the world (see http://aeronet.gsfc.nasa.gov/ for more information). In addition to aerosol optical thickness (AOT), aerosol properties (size distribution and single scattering albedo) in the Level 2 AERONET inversion product (Dubovik and King, 2000) for April 10–12 were also used in this study. The most reliable inversion product is obtained when AOT at 440 nm is greater than 0.4, a condition met on only April 11.

3. Results and discussion

3.1. Flight plan and variation in air pollution

We chose flight plans according to weather conditions. On April 5, 7, 10, and 11, the aircraft made spiral ascents from nearly 300 m up to 4000 m altitude over selected locations south and north of Shenyang, roughly 100 km away from the city center. On April 7 and 9, the aircraft was on cloud seeding missions and flew through clouds at ~3000–4000 m. On April 12, the aircraft circled the Shenyang metropolitan area at ~1000 m.

As seen from Fig. 1, air pollution over the region featured strong day-to-day variation during the experiment. Below 1000–1500 m altitude, or generally within the daytime planetary boundary layer (PBL), flights on April 1, 5, and 11 measured up to 20 ppbv of SO_2 near the surface and ~10 ppbv at ~1000 m, as stagnant conditions prevented dispersion (April 1 and 11) or strong surface winds brought pollution from the region to the south of Shenyang (April 5). Meteorological records suggest that these flights were conducted with a low pressure system approaching the area from the west, and in general represent prefrontal conditions. On April 7, 10, and 12, the flight area was influenced by strong northerly winds and high pressure systems. These postfrontal flights recorded much smaller SO_2 concentration (less than 5 ppbv near the surface). On April 6 and 9, two rainy days, SO_2 was likely reduced by wet removal processes. Above the PBL, the SO_2 concentration was generally low, but substantial SO_2 (~2–3 ppbv) was measured at 2000–3000 m on April 5. Propelled by strong westerly winds in the free troposphere (FT), the observed SO_2 and other pollutants at this altitude can travel far downwind, and a more detailed discussion can be found in our previous studies (Dickerson et al., 2007; Li et al., 2010a). Column integrated SO_2 varied from 0.1 to 0.2 Dobson Unit (DU) on April 7 and 10 to 1–2 DU on April 1 and 5 (Krotkov et al., 2008), demonstrating an order of magnitude change in just days. In the following section, we discuss flights on April 10 and 11 in greater detail to further illustrate the influence of weather conditions on air quality.

3.2. Airborne observation of a pollution event

3.2.1. Overview of the synoptic weather conditions

An overview of the synoptic conditions from April 9 to 12, 2005 is given in Fig. 2. At 0 UTC on April 9, two low pressure systems (or mid-latitude cyclones) were located south (32°N, 120°E) and north–northwest (48°N, 116°E) of Shenyang (Fig. 2a). They traveled eastward in the next 24 h, producing precipitation over the northeastern part of China and moving to the east of Shenyang on April 10 (Fig. 2b). Meanwhile, a high-pressure system centered near the China–Mongolia border began to settle into our flight area, bringing northwest winds with speeds as high as 6 m s^{-1} near the surface. The strong winds lasted until the evening of April 10. By April 11, the two lows and the high mentioned above had moved farther east, with the lows now in the northern Pacific (32°N, 135°E, and 45°N, 150°E) and the center of the high situated just east of the

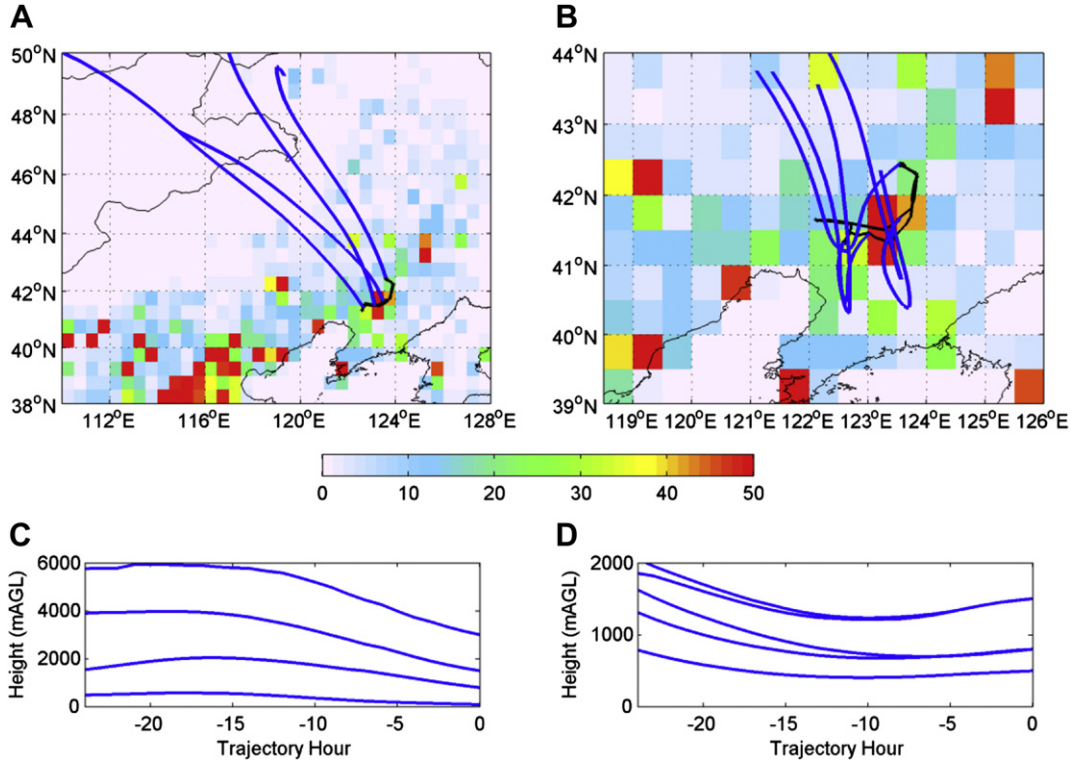

Fig. 3. Flight tracks (solid black line, the upper panel) on (a) April 10 and (b) 11, 2005. Color represents estimated SO_2 emissions (10^3 ton/grid/year, Zhang et al., 2009). Solid blue lines are 24-hr back trajectories calculated every hour along the flight track. Lower panels show the height (above ground level) of the trajectories. (For interpretation of the references to colour in this figure legend, the reader is referred to the web version of this article.)

Korean Peninsula (40°N, 130°E). Another mid-latitude cyclone moved into the region from the west, with its center located to the north of Shenyang (55°N, 125°E). At the surface level, a trough can be found just west of our flight area. Meteorological observations point to stagnant conditions close to the surface (variable wind direction and wind speed < 2 m s^{-1}).

3.2.2. Flight routes and back trajectories

The Y-12 aircraft took similar routes on April 10 and 11 (see Fig. 3 for the flight tracks). On both days, it took off from the airport at around 10 am LST (local standard time), and made two slow spiral ascents from 200–300 m to 4000 m altitude over agricultural fields, one northeast of Shenyang (42.5°N 123.6°E), and the other southwest of the city (41.4°N 122.6°E), before landing between 1:30 and 2:00 pm LST. The main difference between the two flights was that on April 10 the aircraft first flew to the north, while on April 11 it first flew to the south.

Back trajectories at different altitudes along the flight tracks were calculated using the NOAA Air Resource Lab (ARL) HYSPLIT back-trajectory model (Draxler and Rolph, 2003) and NCEP global reanalysis data (Fig. 3). On April 10, there was generally descending flow from the northwest associated with the high pressure system located west of the area. A sounding profile obtained at 8 pm LST revealed an inversion layer at ~1500 m, presumably due to subsidence induced by the high. A layer of scattered fair weather cumulus clouds was observed at roughly the same level during the flight. Trajectories for April 11 indicated that flow was from south or southwest at lower levels (500, 800, and 1500 m above ground level, AGL), and from northwest at higher levels (3000 m AGL).

3.2.3. Altitude profiles of SO_2 and aerosol scattering coefficients

Figs. 4 and 5 present the vertical profiles of SO_2, aerosol scattering coefficients (b_{sp}), temperature, and relative humidity (RH) measured on April 10 and 11.

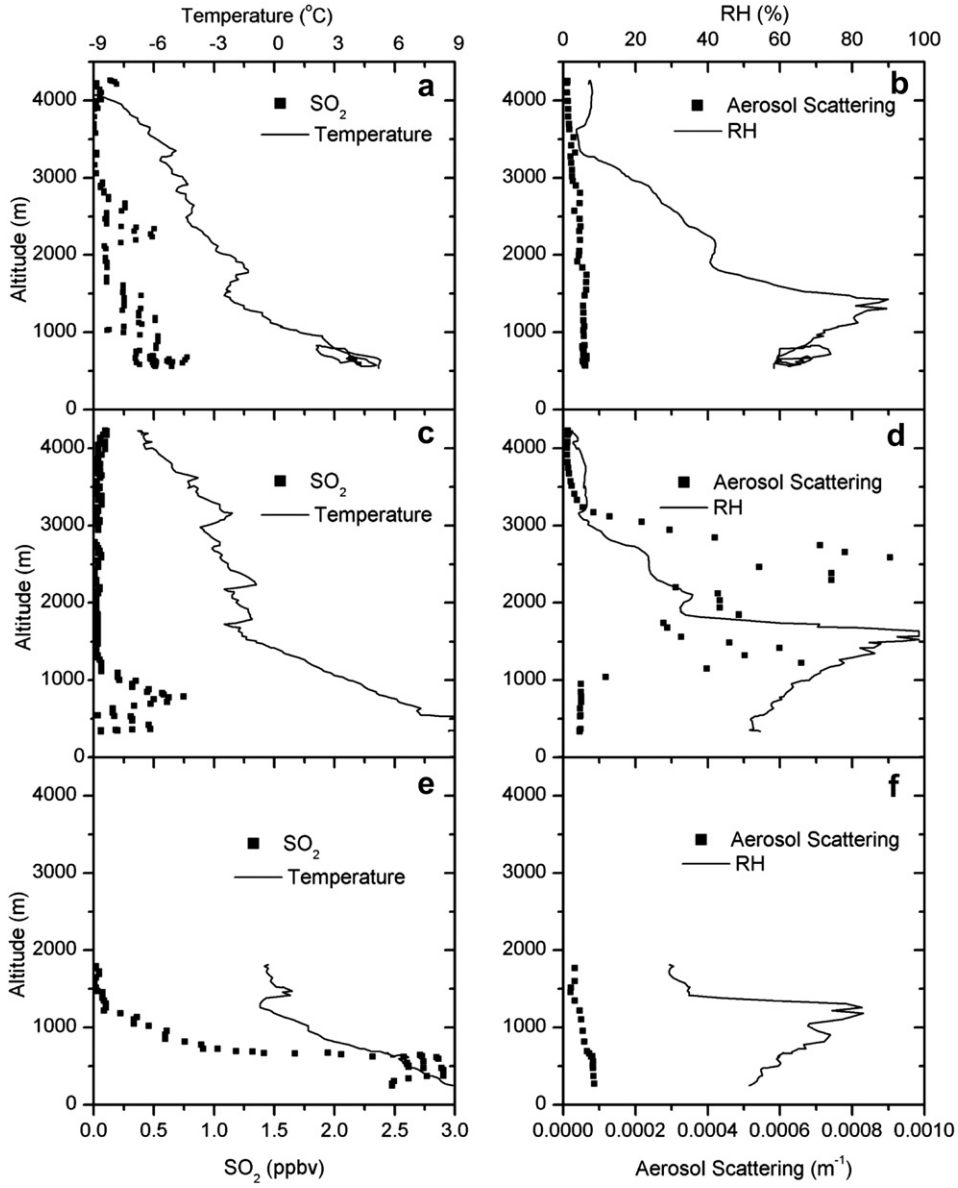

Fig. 4. Altitude profiles of SO_2, temperature, aerosol scattering coefficients (550 nm) and relative humidity on April 10, 2005, measured (a–b) north of Shenyang (42.48°N 123.61°E), (c–d) south of Shenyang (41.37°N 122.61°E), and (e–f) near the airport (41.64°N 123.49°E).

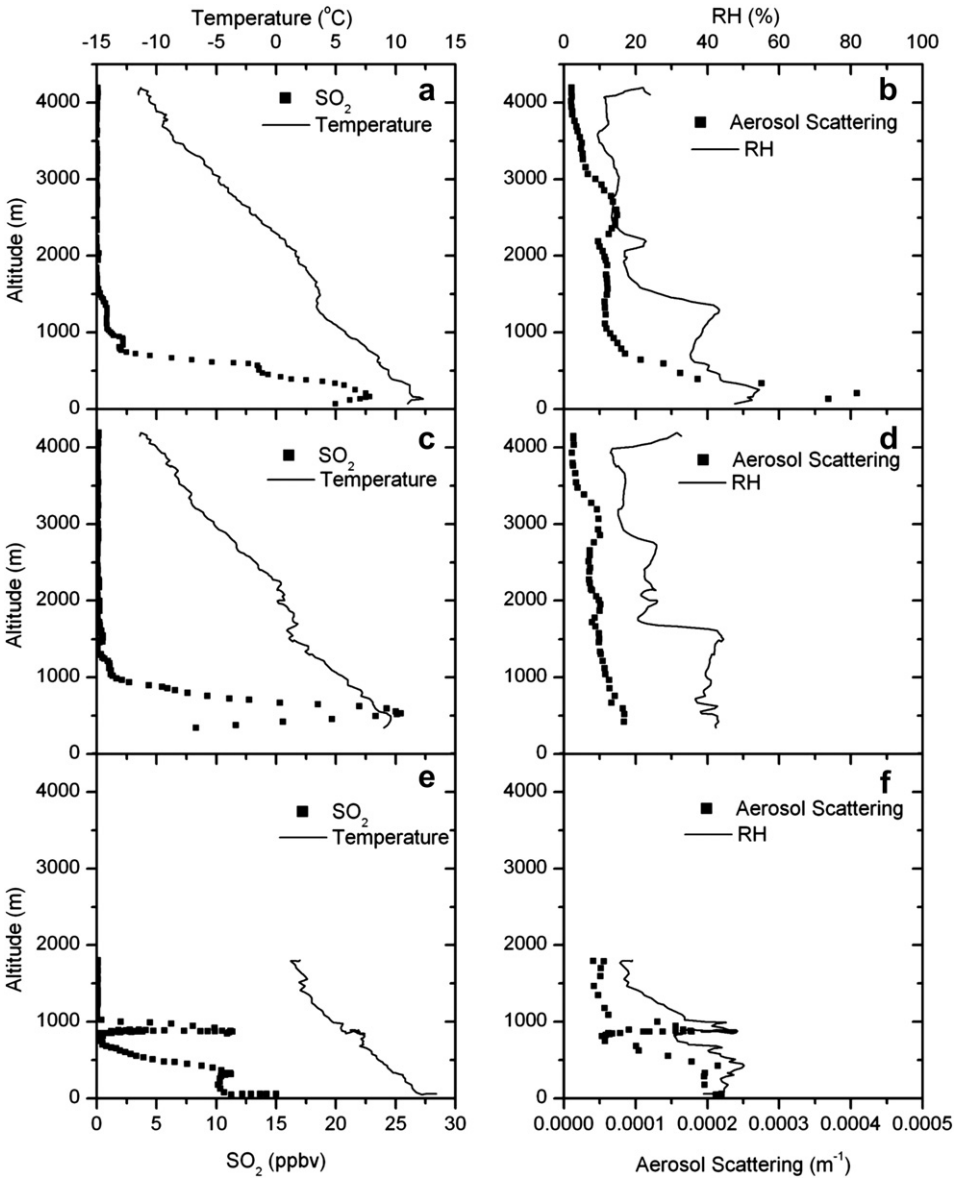

Fig. 5. Altitude profiles of SO_2, temperature, aerosol scattering coefficients (550 nm) and relative humidity on April 11, 2005, measured (a–b) south of Shenyang (41.35°N 122.65°E), (c–d) north of Shenyang (42.45°N 123.61°E), and (e–f) near the airport (41.64°N 123.49°E).

The previously mentioned inversion layer at ~1500 m on April 10 can be identified in all three profiles in Fig. 4. Below this inversion layer or within the PBL, RH increased with height from about 50% at 500 m to almost 100% at 1500 m, where a layer of cumulus clouds existed. Above the inversion layer in the lower free troposphere, RH dropped by 50% in just a few hundred meters. A few more inversion layers can be found between 2000 and 3500 m, likely due to the subsidence associated with the high west of the region. The SO_2 concentration was modest at all altitudes, only ~1 ppbv within the PBL and almost undetectable in the FT. A SO_2 mixing ratio of ~3 ppbv was measured near the airport (Fig. 4e), which is only 20 km away from the city and may at times be influenced by urban plumes.

Aerosol scattering coefficients were $0.5–1 \times 10^{-5}\ m^{-1}$ within the PBL and less than $0.5 \times 10^{-5}\ m^{-1}$ aloft. Peaks as large as $8 \times 10^{-4}\ m^{-1}$ were encountered at 1000–3000 m southwest of Shenyang (Fig. 4d), when the aircraft was flying through the cloud deck. Clouds may bias the measured b_{sp}, although greater RH (e.g., Jeong et al., 2007) and cloud processing (e.g., Wurzler et al., 2000) can enhance aerosol scattering or emit new aerosol particles.

The SO_2 profiles on April 11 were distinctly different (Fig. 5). The top of the PBL during this flight could be identified as an inversion layer (with sudden drop in RH) at ~1500 m. Above the PBL, SO_2 was less than 1 ppbv. Within the PBL, the maximum concentration exceeded 20 ppbv. At 500 m, SO_2 was greater than 10 ppbv in all three profiles. Aerosol scattering coefficients ranged between 1×10^{-4} and $4 \times 10^{-4}\ m^{-1}$ within the PBL, and were generally less than $1 \times 10^{-4}\ m^{-1}$ in the FT. An interesting feature in the FT was the small peaks in b_{sp} at ~2500–3500 m, which suggested possible dust transport from the west. The vertical distribution of aerosols observed during the experiment is further discussed in Section 3.3.

3.2.4. *Accumulation of SO_2 within 24 h from April 10 to 11*

The calculated SO_2 column amounts between 500 and 1000 m altitude on April 11 (0.3–0.6 DU) were more than an order of magnitude higher than those on the previous day (0.02–0.04 DU).

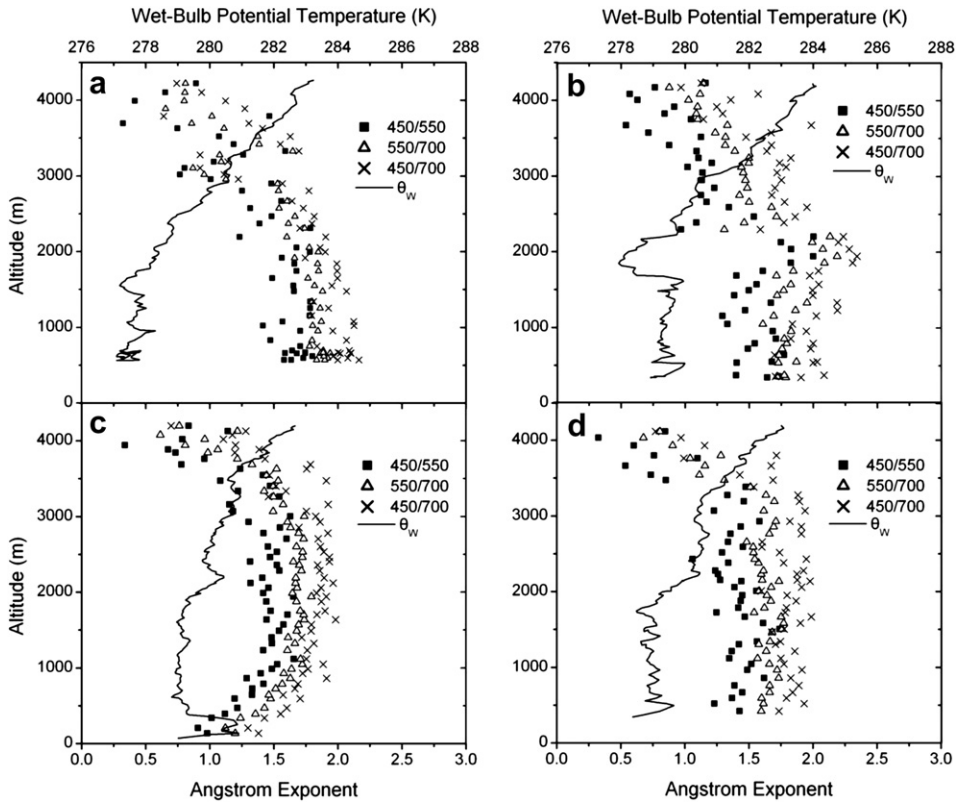

Fig. 6. Altitude profiles of Ångström exponents (AE) and wet-bulb potential temperature on (upper) April 10 and (lower) 11, 2005. Because of preferential loss of large particles in sampling, AE measured from the aircraft represents an upper limit.

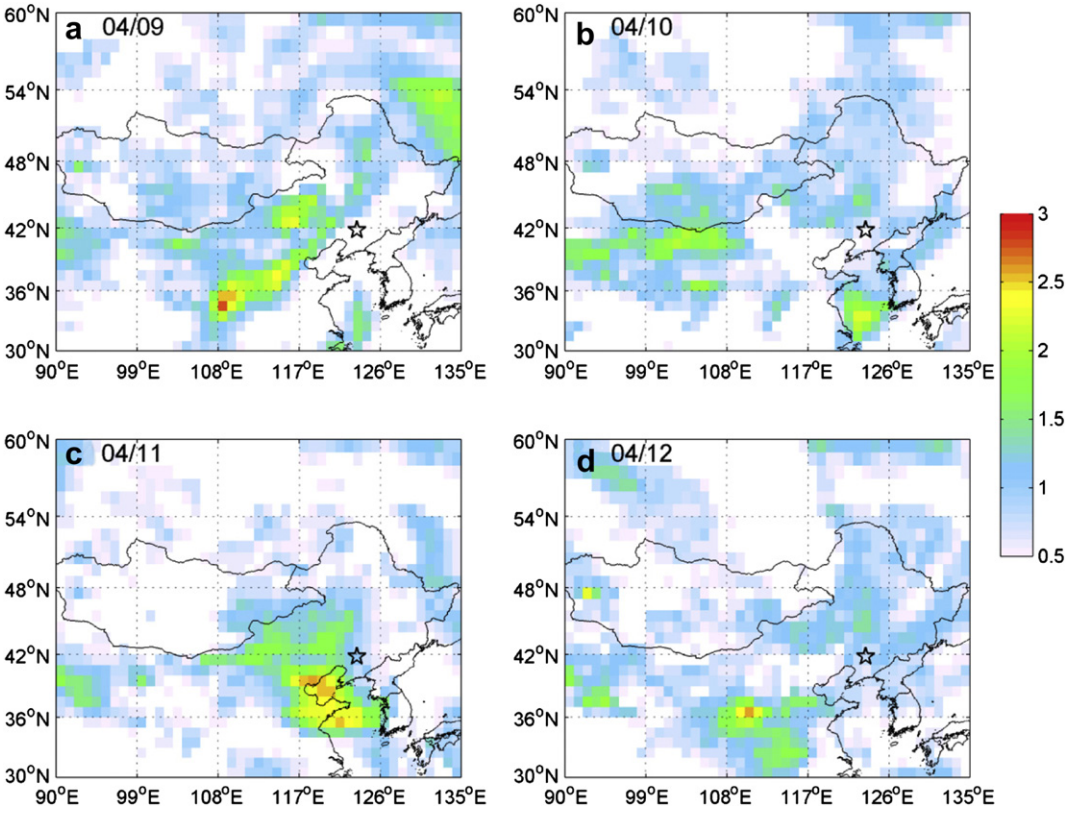

Fig. 7. Aerosol Index from the Ozone Monitoring Instrument onboard the NASA Aura satellite for April 9–12, 2005. Star represents the approximate location of Shenyang.

Since the spiral ascents were made over rural areas containing no significant point sources, this large difference was most likely caused by change in weather conditions. On April 10, strong surface winds (~6 m s^{-1}) favored the dispersion of pollutants emitted within our study area. The region to the northwest has weaker pollution sources (see Fig. 3 for the spatial distribution of SO_2 sources), and northwesterly winds brought relatively clean air into the flight area. In addition, precipitation on April 9 likely decreased the pollutant level across the region. In comparison, stagnant conditions on April 11 suppressed the ventilation of locally emitted pollutants, leading to much greater SO_2 concentration. Trajectory analysis (Fig. 3b) shows that air parcels spent several hours over areas of strong emissions around Shenyang, before being encountered by the aircraft.

The observed increase of SO_2 over the 24 h period between the two flights reflects the strength of the emission sources in the flight area. Assuming our SO_2 profiles are representative of the whole area (40–43°N, 122–125°E), the mass of the total accumulated SO_2 from the April 10 to 11 was approximately 2300 tons, which was greater than but comparable to the daily emission rate of ~1500 ton day^{-1} estimated from energy use data (Streets et al., 2003; Zhang et al., 2009). In this case, strong local emissions combined with weather conditions were conducive to the rapid buildup of surface pollution, leaving the local population particularly vulnerable.

3.3. Size distribution and vertical distribution of aerosols

The Ångström exponent (AE), a parameter reflecting the wavelength dependence of aerosol scattering coefficients, is often used qualitatively to infer the size of aerosol particles (e.g., Eck et al., 1999). Smaller AE values correspond to overall larger particles. In Fig. 6, we present the profiles of AE and wet-bulb potential temperature (θ_w), calculated following Bolton (1980). It should be noted that due to the anticipated sampling losses of large particles, AE in Fig. 6 is likely an upper limit (L. Brent, personal communication, July 2012).

In all four profiles, θ_w varied little within the PBL (below ~1500 m), except within the lowest a few hundred meters on April 11 (Fig. 6c). In the FT (above ~2000 m), θ_w generally increased with height. Ozone was ~50–70 ppbv in the FT, and ~20–40 ppbv within the PBL. The moderate O_3 and low SO_2 (<1 ppbv) concentrations suggested that the FT air sampled on April 10–11 likely originated from even higher layers in the atmosphere, and was not strongly influenced by anthropogenic sources. Photochemical ozone production was weak in this period apparently due to moderate temperatures and insolation. Back trajectories (Fig. 3) indicated that the FT air was from the region to the west of Shenyang, including important dust source regions such as the Gobi deserts. As a result of dust transport from the west, AE in the FT was relatively small at ~0.5–1.5, implying overall larger particles. Greater AE values (~1.5–2) within the PBL indicate finer particles primarily from industrial and other anthropogenic sources such as sulfate and black carbon. Locally emitted soil particles likely contributed to the small AE (~1) observed near the surface (below 200 m) in Fig. 6c.

The remotely sensed Aerosol Index (AI, Hsu et al., 1996) from satellite sensors is most sensitive to elevated, light absorbing aerosols including dust particles. As shown in Fig. 7, moderate to high values of AI (>1.5) were frequently observed over northern China during our experiment regardless of the pollution level near the surface. This suggests that dust can be prevalent over the region in spring. A number of studies have attempted to link satellite-retrieved AOT to surface aerosol mass concentration over China (e.g., Li et al., 2011). Such efforts should account for the different vertical profiles of both anthropogenic and dust aerosols.

Presented in Fig. 8 are the aerosol volume size distributions retrieved from the AERONET Cimel observations on April 10–12, 2005. April 11 was the only day with AOT greater than 0.4 at 440 nm, and the retrievals for this day were more reliable (*cf.* Section 2). While the aerosol loading varied substantially, the size distributions on the three days were similar, with one peak in the accumulation mode (~0.1–0.2 μm in radius) and one larger peak in the coarse mode (~2–3 μm in radius). This bimodal aerosol size distribution is consistent with the aircraft data, which, as already discussed, pointed to the existence of both fine and coarse particles over the area. The AERONET-retrieved single scattering albedo (SSA) in the visible range was 0.92 on April 11, lower than the value (~0.95) determined for dust-dominant aerosols by surface in-situ measurements near the Gobi deserts in northwestern China (Li et al., 2010b). Given the SSA and AE values (0.68–0.75), aerosols over the area likely included both dust and black carbon on April 11.

In Fig. 9, we compare the statistics of Ångström exponents from this experiment with those measured over the eastern U.S. through about 150 summertime flights in three years using the same instrument (Taubman et al., 2006). The Ångström exponents over China were significantly smaller than over the eastern U.S. at all levels. With the exception of few layers, the 75th percentiles of China data were smaller than or comparable to the 25th percentiles of U.S. data. Aerosols over the eastern U.S. in summer were predominantly in the fine mode (e.g., Taubman et al., 2004, 2006). Much smaller AE values measured over China pointed to overall larger aerosol particles compared to the U.S.

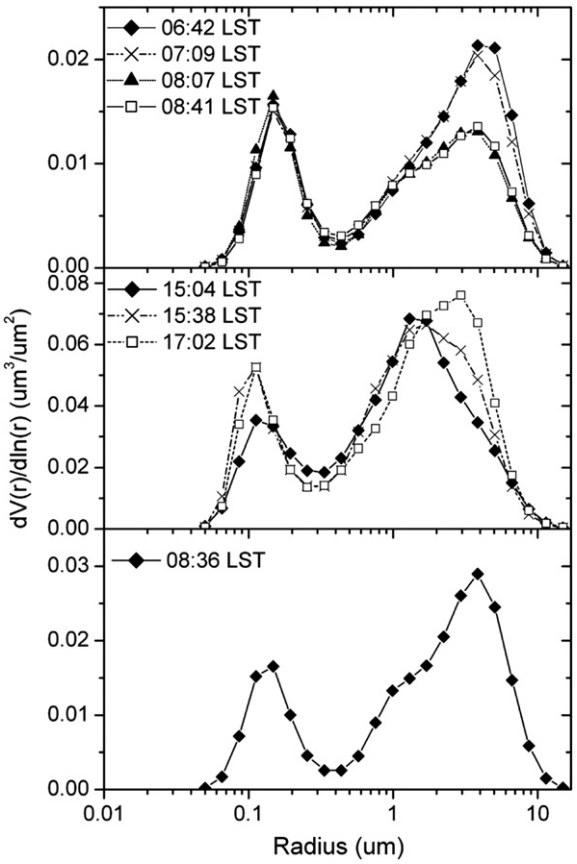

Fig. 8. Aerosol volume size distributions retrieved from AERONET observations south of Shenyang (41.51°N, 122.70°E) on (upper) April 10, (middle) 11, and (lower) 12, 2005. Note the different scales in *Y*-axis for the three days.

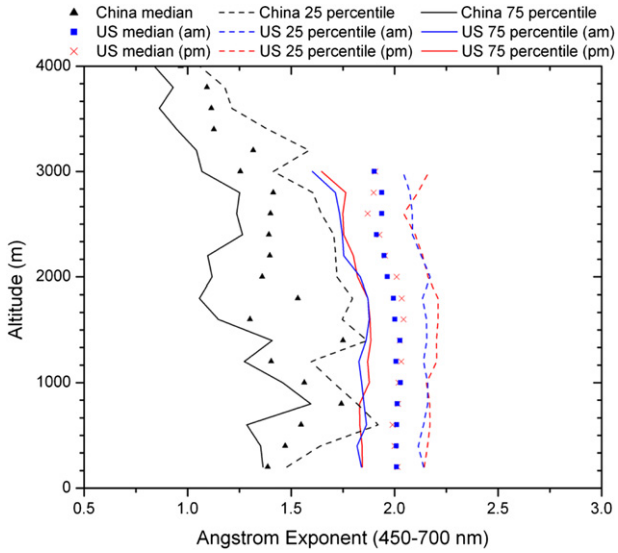

Fig. 9. Altitude profiles of Ångström exponents observed from aircraft flights over eastern China in spring and over the eastern U.S. in summer.

Table 1
Statistics of Ångström exponents (440–675 nm) in 2005 at three AERONET sites in China and the U.S.

Site	Period (DOY: day of year)	25th percentile	Median	75th percentile	Mean	Standard deviation
GSFC[a]	97–120	1.39	1.75	1.86	1.62	0.30
Liaozhong[b]		0.43	0.82	1.20	0.81	0.42
Xianghe[c]		0.60	0.86	0.97	0.78	0.28
GSFC	97–186	1.45	1.75	1.88	1.68	0.28
Liaozhong		0.78	0.97	1.23	0.96	0.32
Xianghe		0.82	1.06	1.22	1.00	0.30
GSFC	1–365	1.57	1.78	1.94	1.74	0.30
Xianghe		0.89	1.12	1.28	1.07	0.27

[a] GSFC: 38.992°N, 76.840°W, AOT (500 nm) = 0.27 ± 0.17 (mean ± std. dev.) during DOY 97–186 in 2005.
[b] Liaozhong: 41.512°N, 122.701°E, AOT (500 nm) = 0.73 ± 0.62 (mean ± std. dev.) during DOY 97–186 in 2005.
[c] Xianghe: 39.754°N, 116.962°E, AOT (500 nm) = 0.76 ± 0.63 (mean ± std. dev.) during DOY 97–186 in 2005.

AERONET observations in northern China and the eastern U.S. show similar differences in AE. Table 1 gives the statistics of AE observed at three sites, with one located in our flight area (Liaozhong) and another in the flight region over the U.S. (GSFC). AERONET measured Ångström exponents were smaller than aircraft measured values, since the latter were likely an upper limit of true AE values. On the other hand, in agreement with the aircraft data, AERONET measurements indicated significantly smaller AE values over China. The annual mean AE in Xianghe is greater than the springtime mean, due to reduced dust activity in other seasons. But even in summer, the AE values in Xianghe were around unity, suggesting the existence of a nontrivial coarse mode. Ground-based, satellite, and aircraft measurements from this experiment together suggest that aerosols over northern China likely have a substantial coarse mode, particularly at elevated heights.

4. Conclusions

Aircraft measurements of SO_2 and aerosol scattering coefficients were made over Shenyang, China in the spring of 2005, under a variety of weather conditions. SO_2 levels were observed to increase by an order of magnitude over the area in a 24 h time period. Little SO_2 was measured on April 10, due to strong northwesterly winds near the surface facilitating the dissipation of pollutants. On the following day, a mid-latitude cyclone began to influence the area, leading to a weak southerly flow and stagnant conditions conducive to the observed SO_2 buildup and demonstrating that high emission rates leave the local population vulnerable to unfavorable weather. Such dramatic fluctuations in pollutant levels due to changes in synoptic conditions have been previously documented in eastern China on the ground (e.g., Wang et al., 2004; Li et al., 2007b), but airborne measurements show that the pollutants can reach substantial altitudes and may have far-reaching effects. Future studies on the influence of weather conditions on similar events may help develop mitigation strategies.

Airborne observations in this study were supplemented by co-located AERONET sun photometer measurements. Aircraft data, ground-based remote sensing, and satellite observations provided a consistent picture of aerosol size distribution and vertical profiles during the experiment. Within the PBL, fine particles of anthropogenic origins dominated while above the PBL, dust transport from the west was more important, and should be accounted for in the satellite remote sensing of surface aerosol pollution. Comparisons of both aircraft and AERONET measurements for the eastern U.S. and China show that the Ångström exponents over China were significantly smaller, implying the prevalence of dust particles in northern China, especially at higher altitudes. There currently exist about 460 AERONET stations around the world (http://aeronet.gsfc.nasa.gov), but few are accompanied by measurements of aerosol vertical distribution, which is important for understanding both the air quality and climate impacts of atmospheric aerosols. Experiments like this one will help characterize aerosol optical and physical properties over China that are essential for better understanding aerosol sources, composition, and variations, and for eventually revealing their effects on dynamic and climatic processes.

Acknowledgments

The study is supported by grants from MOST (2013CB955804), NSF (ATM0412040, AGS1118325) and DOE (DESC0007171). We thank the University of Wyoming (http://weather.uwyo.edu/upperair/sounding.html) for the sounding data used in this study, and D. Giles of NASA/GSFC for comments on the manuscript. We also thank Principal Investigators for establishing and maintaining AERONET sites.

References

Anderson, T.L., Ogren, J.A., 1998. Determining aerosol radiative properties using the TSI 3563 Integrating Nephelometer. Aerosol Science and Technology 29, 57–69.
Bey, I., Jacob, D.J., Logan, J.A., Yantosca, R.M., 2001. Asian chemical outflow to the Pacific in spring: origins, pathways, and budgets. Journal of Geophysical Research 106 (D19), 23097–23114. http://dx.doi.org/10.1029/2001JD000806.
Bolton, D., 1980. The computation of equivalent potential temperature. Monthly Weather Review 108, 1046–1053.
Chen, Y., Zhao, C., Zhang, Q., Deng, Z., Huang, M., Ma, X., 2009. Aircraft study of mountain chimney effect of Beijing, China. Journal of Geophysical Research 114, D08306. http://dx.doi.org/10.1029/2008JD010610.
Dickerson, R.R., Li, C., Li, Z., Marufu, L.T., Stehr, J.W., McClure, B., Krotkov, N., Chen, H., Wang, P., Xia, X., Ban, X., Gong, F., Yuan, J., Yang, J., 2007. Aircraft observations of dust and pollutants over northeast China: insight into the meteorological mechanisms of transport. Journal of Geophysical Research 112, D24S90,. http://dx.doi.org/10.1029/2007JD008999.
Ding, A., Wang, T., Xue, L., Gao, J., Stohl, A., Lei, H., Jin, D., Ren, Y., Wang, X., Wei, X., Qi, Y., Liu, J., Zhang, X., 2009. Transport of north China air pollution by midlatitude cyclones: case study of aircraft measurements in summer 2007. Journal of Geophysical Research 114, D08304. http://dx.doi.org/10.1029/2008JD011023.
Draxler, R.R., Rolph, G.D., 2003. HYSPLIT (HYbrid Single-Particle Lagrangian Integrated Trajectory) Model Access via NOAA ARL READY Website. NOAA Air

Resources Laboratory, Silver Spring, MD. htttp://www.arl.noaa.gov/ready/hysplit4.html.
Dubovik, O., King, M.D., 2000. A flexible inversion algorithm for retrieval of aerosol optical properties from Sun and sky radiance measurements. Journal of Geophysical Research 105, 20673–20696.
Eck, T.F., Holben, B.N., Reid, J.S., Dubovik, O., Smirnov, A., O'Neill, N.T., Slutsker, I., Kinne, S., 1999. Wavelength dependence of the optical depth of biomass burning, urban and desert dust aerosols. Journal of Geophysical Research 104, 31,333–31,350.
Hao, M.-J., Zhao, Y., Zhang, L., Qiao, Z., Xue, B., 2006. Environmental protection measure and countermeasure during the eleventh Five-Year in Shenyang. Environmental Protection Science 32 (3), 52–54 (in Chinese).
Hatakeyama, S., Takami, A., Wang, W., Tang, D., 2005. Aerial observation of air pollutants and aerosols over Bo Hai, China. Atmospheric Environment 39, 5893–5898.
He, H., Li, C., Loughner, C.P.P., Li, Z., Krotkov, N.A., Yang, K., Wang, L., Zheng, Y., Bao, X., Zhao, G., Dickerson, R.R., 2012. SO_2 over central China: measurements, numerical simulations and the tropospheric sulfur budget. Journal of Geophysical Research 117, D00K37. http://dx.doi.org/10.1029/2011JD016473.
He, K., Huo, H., Zhang, Q., 2002. Urban air pollution in China: current status, characteristics, and progress. Annual Review of Energy and the Environment 27, 397–431.
Holben, B.N., Eck, T.F., Slutsker, I., Tanré, D., Buis, J.P., Setzer, A., Vermote, E., Reagan, J.A., Kaufman, Y., Nakajima, T., Lavenu, F., Jankowiak, I., Smirnov, A., 1998. AERONET – a federated instrument network and data archive for aerosol characterization. Remote Sensing of Environment 66, 1–16.
Hsu, N.C., Herman, J.R., Bhartia, P.K., Seftor, C.J., Torres, O., Thompson, A.M., Gleason, J.F., Eck, T.F., Holben, B.N., 1996. Detection of biomass burning smoke from TOMS measurements. Geophysical Research Letters 23, 745–748.
Huebert, B.J., Bates, T., Russell, P.B., Shi, G., Kim, Y.J., Kawamura, K., Carmichael, G., Nakajima, T., 2003. An overview of ACE-Asia: strategies for quantifying the relationships between Asian aerosols and their climatic impacts. Journal of Geophysical Research 108 (D23), 8633,. http://dx.doi.org/10.1029/2003JD003550.
Jacob, D.J., Crawford, J.H., Kleb, M.M., Connors, V.S., Bendura, R.J., Raper, J.L., Sachse, G.W., Gille, J.C., Emmons, L., Heald, C.L., 2003. Transport and Chemical Evolution over the Pacific (TRACE-P) aircraft mission: design, execution, and first results. Journal of Geophysical Research 108 (D20), 9000. http://dx.doi.org/10.1029/2002JD003276.
Jeong, M.-J., Li, Z., Andrews, E., Tsay, S.-C., 2007. Effect of aerosol humidification on the column aerosol optical thickness over the Atmospheric Radiation Measurement Southern Great Plains site. Journal of Geophysical Research 112, D10202. http://dx.doi.org/10.1029/2006JD007176.
Krotkov, N.A., McClure, B., Dickerson, R.R., Carn, S.A., Li, C., Bhartia, P.K., Yang, K., Krueger, A.J., Li, Z., Levelt, P.F., 2008. Validation of SO_2 retrievals from the ozone monitoring instrument over NE China. Journal of Geophysical Research 113, D16S40. http://dx.doi.org/10.1029/2007JD008818.
Li, Z., Chen, H., Cribb, M., Dickerson, R., Holben, B., Li, C., Lu, D., Luo, Y., Maring, H., Shi, G., Tsay, S.-C., Wang, P., Xia, X., Zheng, Y., Yuan, T., Zhao, F., 2007a. Preface to special section on East Asian studies of Tropospheric Aerosols: An International Regional Experiment (EAST-AIRE). Journal of Geophysical Research 112, D22S00. http://dx.doi.org/10.1029/2007JD008853.
Li, C., Marufu, L.T., Dickerson, R.R., Li, Z., Wen, T., Wang, Y., Wang, P., Chen, H., Stehr, J.W., 2007b. In situ measurements of trace gases and aerosol optical properties at a rural site in northern China during East Asian Study of Tropospheric Aerosols: an International Regional Experiment 2005. Journal of Geophysical Research 112, D22S04. http://dx.doi.org/10.1029/2006JD007592.
Li, C., Krotkov, N.A., Dickerson, R.R., Li, Z., Yang, K., Chin, M., 2010a. Transport and evolution of a pollution plume from northern China: a satellite-based case study. Journal of Geophysical Research 115, D00K03. http://dx.doi.org/10.1029/2009JD012245.
Li, C., Tsay, S.-C., Fu, J.S., Dickerson, R.R., Ji, Q., Bell, S.W., Gao, Y., Zhang, W., Huang, J., Li, Z., Chen, H., 2010b. Anthropogenic air pollution observed near dust source regions in northwestern China during springtime 2008. Journal of Geophysical Research 115, D00K22. http://dx.doi.org/10.1029/2009JD013659.
Li, C., Hsu, N.C., Tsay, S.-C., 2011. A study on the potential applications of satellite data in air quality monitoring and forecasting. Atmospheric Environment 45, 3663–3675.
Luke, W.T., 1997. Evaluation of a commercial pulsed fluorescence detector for the measurement of low-level SO_2 concentrations during the gas-phase sulfur intercomparison experiment. Journal of Geophysical Research 102, 16255–16265.
Ma, J., Chen, Y., Wang, W., Yan, P., Liu, H., Yang, S., Hu, Z., Lelieveld, J., 2010. Strong air pollution causes widespread haze-clouds over China. Journal of Geophysical Research 115, D18204. http://dx.doi.org/10.1029/2009JD013065.
Parrish, D.D., Kondo, Y., Cooper, O.R., Brock, C.A., Jaffe, D.A., Trainer, M., Ogawa, T., Hübler, G., Fehsenfeld, F.C., 2004. Intercontinental transport and chemical transformation 2002 (ITCT 2K2) and pacific exploration of Asian continental emission (PEACE) experiments: an overview of the 2002 winter and spring intensives. Journal of Geophysical Research 109, D23S01. http://dx.doi.org/10.1029/2004JD004980.
Streets, D.G., Bond, T.C., Carmichael, G.R., Fernandes, S.D., Fu, Q., He, D., Klimont, Z., Nelson, S.M., Tsai, N.Y., Wang, M.Q., Woo, J.-H., Yarber, K.F., 2003. An inventory of gaseous and primary aerosol emissions in Asia in the year 2000. Journal of Geophysical Research 108, 8809. http://dx.doi.org/10.1029/2002JD003093.
Taubman, B.F., Marufu, L.T., Piety, C.A., Doddridge, B.G., Stehr, J.W., Dickerson, R.R., 2004. Airborne characterization of the chemical, optical, and meteorological properties, and origins of a combined ozone-haze episode over the Eastern United States. Journal of Atmospheric Science 61, 1781–1793.
Taubman, B.F., Hains, J.C., Thompson, A.M., Marufu, L.T., Doddridge, B.G., Stehr, J.W., Piety, C.A., Dickerson, R.R., 2006. Aircraft vertical profiles of trace gas and aerosol pollution over the mid-Atlantic United States: statistics and meteorological cluster analysis. Journal of Geophysical Research 111, D10S07. http://dx.doi.org/10.1029/2005JD006196.
Wang, G., Kawamura, K., Hatakeyama, S., Takami, A., Li, H., Wang, W., 2007. Aircraft measurement of organic aerosols over China. Environmental Science and Technology 41, 3115–3120.
Wang, T., Wong, C.H., Cheung, T.F., Blake, D.R., Arimoto, R., Baumann, K., Tang, J., Ding, G.A., Yu, X.M., Li, Y.S., Streets, D.G., Simpson, I.J., 2004. Relationships of trace gases and aerosols and the emission characteristics at Lin'an, a rural site in eastern China, during spring 2001. Journal of Geophysical Research 109, D19S05. http://dx.doi.org/10.1029/2003JD004119.
Wang, W., Ma, J., Hatakeyama, S., Liu, X., Chen, Y., Takami, A., Ren, L., Geng, C., 2006. Aircraft measurements of vertical ultrafine particles profiles over northern China coastal areas during dust storms in 2006. Atmospheric Environment 42, 5715–5720.
Wurzler, S., Reisin, T.G., Levin, Z., 2000. Modification of mineral dust particles by cloud processing and subsequent effects on drop size distributions. Journal of Geophysical Research 105 (D4), 4501–4512.
Xia, X., Chen, H., Li, Z., Wang, P., Wang, J., 2007. Significant reduction of surface solar irradiance induced by aerosols in a suburban region in northeastern China. Journal of Geophysical Research 112, D22S02. http://dx.doi.org/10.1029/2006JD007562.
Xu, Z., Yu, D., Jing, L., Xu, X., 2000. Air pollution and daily mortality in Shenyang, China. Archives of Environmental Health: An International Journal 55 (2), 115–120.
Xue, L., Ding, A., Gao, J., Wang, T., Wang, W., Wang, X., Lei, H., Jin, D., Qi, Y., 2010. Aircraft measurements of the vertical distribution of sulfur dioxide and aerosol scattering coefficient in China. Atmospheric Environment 44, 278–282.
Zhang, Q., Zhao, C., Tie, X., Wei, Q., Huang, M., Li, G., Ying, Z., Li, C., 2006. Characterizations of aerosols over the Beijing region: a case study of aircraft measurements. Atmospheric Environment 40, 4513–4527.
Zhang, Q., Streets, D.G., Carmichael, G.R., He, K.B., Huo, H., Kannari, A., Klimont, Z., Park, I.S., Reddy, S., Fu, J.S., Chen, D., Duan, L., Lei, Y., Wang, L.T., Yao, Z.L., 2009. Asian emissions in 2006 for the NASA INTEX-B mission. Atmospheric Chemistry and Physics 9, 5131–5153.